Switching on the fluorescence emission of polypirydine ligands *via* simultaneous metal and H^+ binding

Luca Conti,[a*] Claudia Giorgi,[a] Barbara Valtancoli[a], Paola Paoli,[b] Patrizia Rossi,[b] Andrea Marchionni,[c] Enrico Faggi,[a] and Andrea Bencini.[a*]

[a] *Department of Chemistry "Ugo Schiff", University of Florence, Via della Lastruccia 3, Florence, 50019-Sesto Fiorentino, Italy*

[b] *Department of Industrial Engineering, University of Florence, Via S. Marta 3, Florence, I-50139, Italy*

[c] *Istituto di Chimica dei Composti OrganoMetallici (ICCOM_CNR) Via Madonna del Piano 10, 50019-Sesto Fiorentino (FI).*

Abstract. The synthesis and characterization of two new open-chain ligands, **L1** and **L2**, featuring a tetraethylenpentaamine chain linking *via* methylene bridges the 6 and 2 positions of two equal 2,2'-bipyridyl (bpy) and 9-methyl-1,10-phenanthroline (9-methyl-phen) moieties, respectively, is reported. Their basicity properties and complexation features toward Cu^{2+}, Zn^{2+}, Cd^{2+} and Pb^{2+} have been studied by means of potentiometric, UV-vis and fluorescence emission measurements in aqueous solution. Both ligands form stable mono- and dinuclear complexes, the metal ion being coordinated by a single bpy or phen unit and the amine groups on the aliphatic chain. Among all the metal ions tested, only the Zn^{2+} complex with **L2** displays an enhanced fluorescence emission at neutral pH, thanks to the simultaneous binding of one Zn^{2+} ion and H^+ ion(s) with the formation in solution of emissive protonated species. Binding of a second metal switches off the emission again.

Keywords. Chemosensors, fluorescence, metal sensing, polyamine.

INTRODUCTION

There is a current interest in the development of chemosensors for cationic species in aqueous solution, in particular metal cations, due to the relevance of most of them in biological and environmental chemistry.[1-6] Fluorescent chemosensors are among the most used, due to their extreme versatility and sensibility in metal detection. They also present the peculiar ability to detect the evolution of the metal concentrations over the time and display great spatial resolution. These properties have been particularly exploited for the analysis of the role of several metal ions, in particular Zn^{2+}, in cell metabolism. However, this requires the formation of stable metal complexes in real matrices and thermodynamic and optical selectivity in metal coordination.

The most common approach to the realization of synthetic molecular chemosensors consists in the design of molecules constituted by a binding unit, linked to a signalling moiety by a spacer (conjugate chemosensors). An accurate tuning of the structural features of the binding unit, the spacer and the fluorophore residue may lead to the development of selective chemosensors for targeted metal cations.[1-10]

In this scenario, polyamine scaffolds represent an intriguing but versatile choice to be employed as binding units for selected metals. In fact, polyamines normally form remarkably stable metal complexes in aqueous solution, in particular with transition metals, and can be easily functionalized at the nitrogen donors, allowing for facile implementation of chemosensors by using the receptor-spacer-fluorophore strategy. At the same time, the presence of hydrophilic amine groups generally ensures high solubility in water to the chemosensors and its complexes, a necessary pre-requisite to obtain metal sensing in aqueous matrices.[6c, 6e, 7a, 8a, 11-13]

A partial drawback in the use of polyamine receptors can be their protonation in water, which can compete with metal binding, limiting the pH range in which polyamine chemosensors can successfully bind and signal the metal cations.[13-17] At the same time, polyamines can afford protonated complexes in aqueous solution, whose formation can affect the fluorescence emission of the complex, changing its intensity and/or its wavelength,[16-21] As a result the signal generated by the chemosensor upon metal binding can be modulated by pH.[12-14]

We have previously reported on the metal coordination and sensing properties in aqueous solution of a series of receptors constituted by a single fluorogenic heteroaromatic unit, in particular 1,10-phenanthroline and 2,2'-dipyridine, inserted within a macrocyclic or linear aliphatic polyamine framework.[8a-d, 22-24] These ligands are often able to signal Zn^{2+} coordination thanks to an enhancement of the emission upon metal binding. However, their sensing properties are influenced by the structural characteristics of the ligand and its Zn^{2+} complexes, including the number and disposition of amine donors, the overall rigidity of the molecular backbone, and, in the case of

macrocyclic ligands, the dimension of the cavity. In these complexes, the heteroaromatic nitrogens are unequivocally bound to the metal cations. However, the stiffening of the macrocyclic structure imposed by the heteroaromatic moieties may not allow the simultaneous coordination to the metal cations of all the nitrogen donors of the binding unit. Interestingly enough, the 'benzylic' amine groups, adjacent to the heteroaromatic unit, are not bound, or weakly bound, to the metal, making their lone pair available to quench the excited state of the fluorophore via an electron transfer process (PET). As a consequence, normally fluorescent Zn^{2+} complexes result to be scarcely emissive.[8a,b, 22-24]

In this paper, we extend this study to two open-chain ligands, **L1** and **L2** in Scheme 1, containing a pentaamine aliphatic chain linked at its extremities to two equal 2,2'-bipyridyl (bpy) or 9-methyl-1,10-phenanthroline (9-methyl-phen) moieties, respectively. Our purpose is the analysis of the effects on both metal binding and sensing of the presence of two fluorogenic units linked by a flexible chain. Therefore, complex stability and fluorescence emission in the presence of metal cations, will be compared to those of the previously reported ligands **L3**[24] and **L4**[8a] (Scheme 1), which contain the same aliphatic pentaamine chain linking the 6,6' and 2,9 positions of a single bpy or phenanthroline (phen) moiety, respectively, and present more rigid structures, due to their macrocyclic architecture. In particular, we focused our attention on the coordination and sensing properties of **L1** and **L2** toward Zn^{2+}, which often form fluorescent complexes with polyamine ligands, Cd^{2+} and Pb^{2+}, which normally give metal complexes with polyamine receptors with similar stability, and Cu^{2+}, as representative example of paramagnetic transition metal cations.

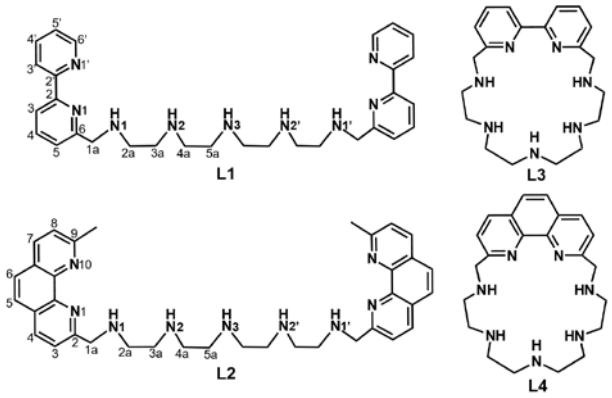

Scheme 1: Drawing of molecular chemosensors herein reported.

RESULTS AND DISCUSSION

Synthesis of ligands. L1 and **L2** were obtained by following a similar procedure, reported in Scheme **2** for **L1** and Scheme S1 for **L2** (Supporting Information)**.** In the case of **L1**, reaction of 6-(bromomethyl)-2,2'-bipyridyl (**1**)[25] and tosylated pentaamine 1,4,7,10,13-pentakis-tosylsulfonyl)-1,4,7,10,13-pentaazatridecane (**2**)[26] in the presence of K_2CO_3 as a base in CH_3CN, affords the pentatosylated compound **3**, which was purified by column chromatography on neutral alumina. Removal of the tosyl groups was then performed in CH_3COOH/HBr mixture in the presence of phenol to avoid oxidation of the reaction product, which was isolated as hydrobromide salt (**L1**·5HBr) by addition of CH_2Cl_2 to the reaction mixture and following recrystallization from EtOH/H_2O. A similar procedure was used to obtain **L2**, replacing **1** with 2-(chloromethyl)-9-methyl-1,10-phenanthroline[27] in the first synthetic step (Scheme S1).

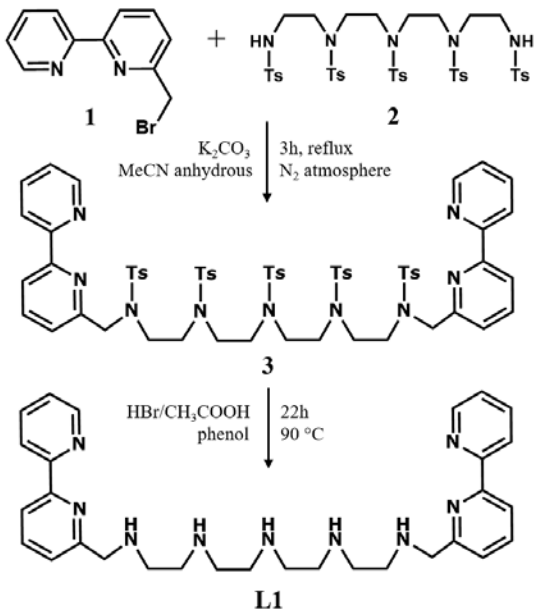

Scheme 2: Schematic route for the synthesis of **L1**

Ligand protonation. Since protonation of polyamine receptors is competitive with the process of metal complexation, we preliminarily carried out a study of the basicity properties of **L1** and **L2** coupling potentiometric, spectrophotometric and fluorimetric measurements in aqueous solutions. The protonation constants of **L1** and **L2**, determined by means of potentiometric measurements in NMe_4Cl 0.1 M are reported in Table 1, while the correspondent distribution diagrams are shown in Figures S11-12.

Table 1: Protonation constants of **L1** and **L2**, determined in aqueous solution NMe_4Cl 0.1 M at 298 ± 0.1 K ([**L1**] = [**L2**] = 1 x 10^{-3} M. Values in parenthesis are standard deviations on the last significant figures.

Equilibrium	Log K[a]	
	L1	**L2**
$L + H^+ = [HL]^+$	9.29(3)	9.1(1)
$[HL]^+ + H^+ = [H_2L]^{2+}$	8.50(2)	8.6(1)
$[H_2L]^{2+} + H^+ = [H_3L]^{3+}$	6.74(3)	7.2(1)
$[H_3L]^{3+} + H^+ = [H_4L]^{4+}$	4.76(5)	4.7(1)
$[H_4L]^{4+} + H^+ = [H_5L]^{5+}$	4.20(4)	4.2(1)
$[H_5L]^{5+} + H^+ = [H_6L]^{6+}$	3.57(5)	3.2(2)
$[H_6L]^{6+} + H^+ = [H_7L]^{7+}$	3.06(4)	2.9(1)

Both ligands behave as heptaprotic bases, being able to bind up to seven protons within the pH range investigated (2-11). As shown in Table 1, the first three protonation constants of **L1** and **L2** are significantly higher than those reported for bpy or phen (log K = 4.35 and 4.96, respectively),[28,29] suggesting that the heteroaromatic nitrogen atoms are not directly involved in these first protonation equilibria. Analysis of UV-vis absorption spectra of receptors at different pH values may provide useful information about the role of the heteroaromatic units in the overall acid-base behaviour of these molecules. In fact, protonation of nitrogen atoms of bpy or phen units causes a red-shift of the corresponding absorption bands, making these spectral changes a diagnostic tool to monitor the protonation state of the heteroaromatic units.[30,31]

As shown in Figure 1a, the characteristic absorption of the bpy unit, centered at ca. 280 nm, results to be almost independent on pH, at least in the pH range 12 - 4.2. Below pH 4.2, a marked red-shift is observed, resulting in the formation of a new sharp band centered a *ca* 305 nm. This absorption band, diagnostic of the formation of the bipyridinium cation,[30] can be attributed to the formation in solution of the hexa- and hepta-protonated species of the ligand, $[H_6\mathbf{L1}]^{6+}$ and $[H_7\mathbf{L1}]^{7+}$, as outlined by the absorbance values at 305 nm superimposed to the distribution diagram of the protonated species of the receptor in aqueous solution (Figure 1b). This indicates that protonation of the heteroaromatic moieties is likely to occur during the two last protonation steps, as expected considering the lower basicity of these heteroaromatic nitrogen atoms with respect to aliphatic ones.[32]

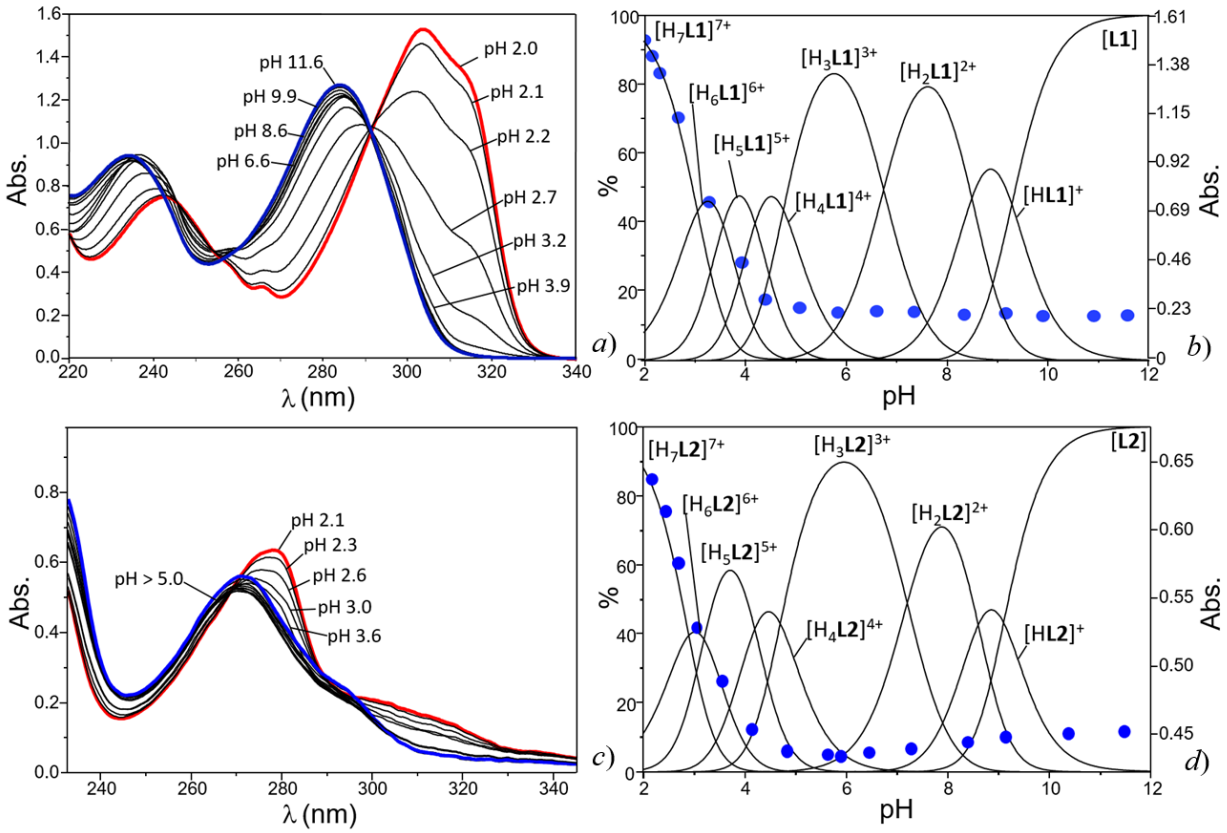

Figure 1: Uv-visible absorption spectra of aqueous solutions of **L1** (a) and of **L2** (c) at different pH values. In figures (b) and (d) are respectively reported the variation of the absorbance at 305 nm (for **L1**) and at 278 nm (for **L2**), as a function of pH, superimposed to the relative distribution diagrams of the species present in solution ([**L1**] = 3.5 x 10^{-5} M, [**L2**] = 1 x 10^{-5} M).

A similar behaviour was also found for **L2** (Figures 1c,d). In fact, the ligand displays the typical band of phen at 268 nm in the pH range 12-5. By decreasing pH from 5 to 2, a red shift of this band, up to 278 nm, is observed, accompanied by the formation of a broad shoulder at 310 nm. These spectral changes can be attributed to protonation of the phen moiety and occur, analogously to **L1**, with the formation in solution of the hexa- and heptaprotonated species $[H_6\mathbf{L2}]^{6+}$ and $[H_7\mathbf{L2}]^{7+}$ (Figure 1d), in keeping with phen protonation in the last two protonation equilibria at strongly acidic pH values.

The interpretation of the acid-base behaviour of ligands by means of spectrofluorimetric measurements is more intriguing, since the emission properties of fluorescent polyamines are generally affected by the protonation equilibria occurring on both the luminescent units as well as on the polyamine moieties.

Bpy is poorly emissive in aqueous solution, at least in its not protonated form (pH > 4), while its protonation induces fluorescence emission at 345 nm.[30] As a consequence, **L1** is basically not emissive in a wide range of pH (11-4) (Figures 2a,b). However, below pH 4 the formation of the hexa- and heptaprotonated species of ligand ($[H_6\mathbf{L1}]^{6+}$, $[H_7\mathbf{L1}]^{7+}$) gives rise to the typical emission

band of the bipyridinium cation with a maximum at 345 nm, confirming the protonation of the heteroaromatic units in the last two protonation steps.

A somewhat different behaviour is found in the case of **L2** (Figures 2c,d).

Phen features a characteristic fluorescence emission band in water, centered at ca. 360 nm, which is red-shifted at 410 nm upon its protonation below pH 5.[30,31] On the other hand, previous works on polyamine macrocycles containing phen moieties have shown that the amine groups, in particular the benzylic ones, closest to the fluorophore, can efficiently quench its fluorescence emission *via* a photoinduced electron-transfer (PET) process from their lone pairs to the excited fluorophores.[8a,8b] Protonation of the amine groups clearly inhibits this process, giving rise to a renewal of the fluorescence emission.

In case of **L2** (Figure 2c,d), the ligand is weakly emissive, displaying a broad band below 400 nm at alkaline pH values, likely due to the PET effect from non-protonated amine groups to the phen moieties. By decreasing pH, the fluorescence emission of the ligand increases up to pH 5.8, where the three-protonated $[H_3\mathbf{L2}]^{3+}$ specie is prevalent in solution (Figure 2d). This effect can be rationalized considering that an increased number of acidic protons gathered on the polyamine chain in $[H_3\mathbf{L2}]^{3+}$ can induce a progressive inhibition of the PET process, with consequent increase of the fluorescence emission of the fluorophore, featuring a broad band with two maxima at 365 and 385 nm.

Further lowering of pH produces a decrease of the intensity of the phen band at 370 nm and the appearance in the spectra of the typical band of the phenanthrolinium cation, whose intensity increases from pH 4.8 to 2. As shown in Figure 2d, the enhancement of the emission at 405 nm is related to the formation in solution of the species with the highest protonation degree, confirming that protonation of the heteroaromatic units occurs in the last protonation steps of the ligand.

Therefore, while the emission of **L1** is only determined by protonation of bpy, in the case of **L2** both the protonation state of the fluorophore and of the polyamine chain affects the fluorescence emission of the ligand.

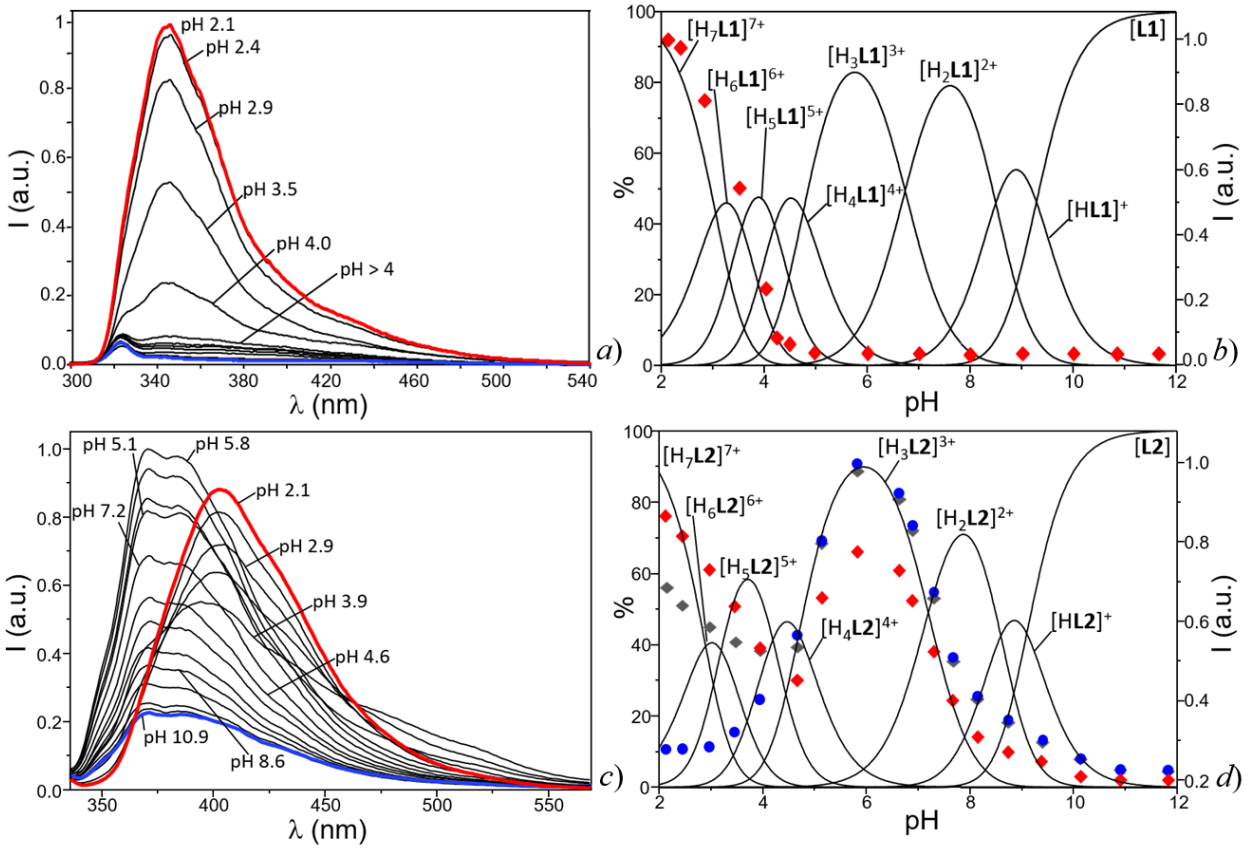

Figure 2: Fluorescence spectra of aqueous solutions of **L1** (a) and **L2** (c) at different pH values. On the right side are reported the variations of the fluorescence emission of **L1** at 345 nm (red squares, (b)), and of **L2** at 365, 385 and 405 nm (blue circles, grey and red squares respectively, (d)) as a function of pH, superimposed to the distribution diagrams of the species present in solution ([**L1**] = [**L2**] = 1.0 x 10^{-5} M, λ_{exc}(**L1**) = 291 nm, λ_{exc}(**L2**) = 295 nm).

The latter consideration prompted us to collect ^{1}H NMR spectra at different pH values, in order to obtain more information on proton localization in the different protonation states of **L2** (Figure 3).

The ligand features two sets of 6 signals in the aliphatic and in the aromatic regions whose pH-dependence is displayed in Figure 3a. The number and integrations of signals accounts for a D_{2h} time averaged symmetry, which is preserved throughout all the pH range investigated. As shown in figure, by decreasing pH from 12 to 8, the resonances of the methylene groups of the ethylenic chains undergo a significant downfield shift, while the shifts of resonances of the benzylic methylene group (a1), the methyl group (CH_3) and the aromatic protons are negligible. Considering that in the pH range 12-8, the $[H_2\mathbf{L2}]^{2+}$ and $[H\mathbf{L2}]^{+}$ species are formed in solution, the observed changes in the resonance shifts suggest that the first two protonation steps do not involve the N1 nitrogen and occur on the aliphatic amine groups N2 and N3, in keeping with their higher basicity. Further pH decrease, up to pH 5, induces a remarkable downfield shifts of the resonance of the benzylic methylene groups a1 (see Scheme 1 for atom labelling). Among the signals of the ethylenic chains, a large downfield shift is observed for a single resonance, which can be attributed

to the a2 hydrogens, adjacent to the benzylic nitrogens. This leads us to suggest that in the $[H_3\mathbf{L2}]^{3+}$, whose formation in solution occurs in the pH range 8-5, the acidic protons are localized on the benzylic amine groups (N1) and on the central nitrogen (N3) of the aliphatic chain of the receptor. In fact, the protonated nitrogens would result separated one from each other by a non-protonated amine residue or the phen unit, ensuring an optimal minimization of the electrostatic repulsion between the positively charged ammonium groups. At the same time, protonation of the benzylic nitrogens would efficiently prevent quenching of the fluorophore emission *via* PET mechanism, in agreement with the result of fluorimetric measurements.

Further decrease of pH (below 5) leads to a further downfield shift of all aliphatic signals, the most relevant being those of the methyl groups CH_3. Significant shifts are observed for the aromatic protons, in particular below pH 4, confirming that protonation of the heteroaromatic nitrogens occurs only in the last protonation steps of the ligand, in agreement with their lower basicity.

The pH dependence of ^1H resonances of **L1** (Figures S13 and S14, Supporting Information) are similar to that reported for **L2**, suggesting a similar proton distribution in the different species of the ligand.

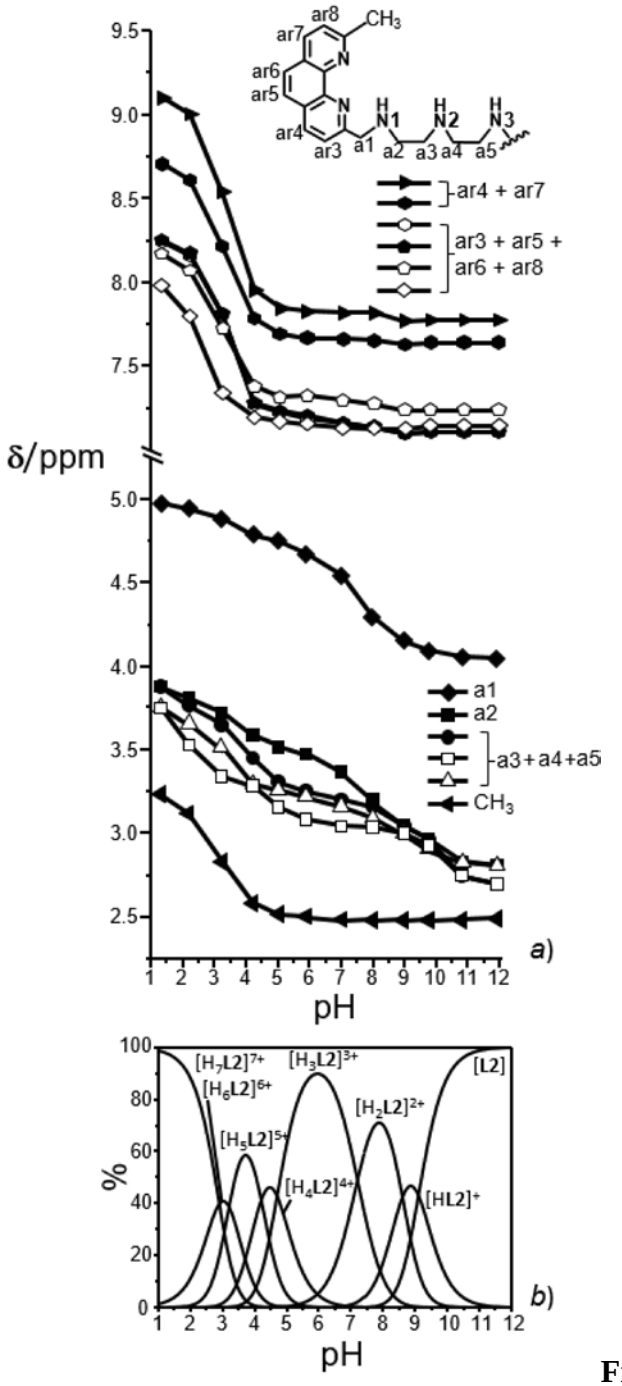

Figura 3 Cambiata

Figure 3: a) pH dependence of the ^{1}H NMR spectroscopic signals of **L2**; b) distribution diagram of the protonated species of **L2** ([**L2**] = 1 x 10^{-3}M, 298 K, 0.1 M NMe_4Cl).

Metal complexation in aqueous solutions. The binding ability of **L1** and **L2** toward Cu^{2+}, Zn^{2+}, Cd^{2+} and Pb^{2+} was first analysed by means of potentiometric titrations in aqueous medium, in order to determine the species present in solution, their formation constants and to establish the possible presence of selectivity patterns among the different metal cations. Unfortunately, in the case of Cd^{2+} and Pb^{2+} complexes with **L1**, the scarce solubility of the complexes in water at the concentrations used for these measurements (*ca* $1{\cdot}10^{-3}$ M) precludes their study by this technique.

The stability constants of metal complexes formed with **L1** and **L2** are reported in Table 2, while the corresponding distribution diagrams of the species formed in solution are reported in Figures S15-S26 (Supporting Information).

Both ligands form stable complexes with ligand to metal 1:1 and 1:2 stoichiometries with all metals under investigation.

Considering the mononuclear complexes, the stability constants of the $[ML]^{2+}$ complexes (M = Cu^{2+}, Zn^{2+} for **L1** and Cu^{2+}, Zn^{2+}, Cd^{2+} and Pb^{2+} for **L2**) are 2-3 logarithmic units higher than those reported for the correspondent metal-complexes with macrocyclic ligands containing a tetraethylenepentamine macrocyclic chain, linked to the 6,6' or 2,9 positions of a bpy or phen unit, respectively (**L3** and **L4** in Scheme 1). We speculate that the higher stability of the mononuclear complexes with the open chain ligands with respect to the corresponding cyclic ones could be related to the higher flexibility of the open-chain polyamine ligands. As a result, **L1** and **L2** can 'wrap' around the coordinated metals, better satisfying the metal coordination requirements to achieve a higher overall metal-ligand interaction and inducing a larger desolvation of the coordinated metal cations. Results from MD simulations (300 K in vacuum and in implicit solvent modeled by using distance dependent dielectric constant set to 80r) performed on the neutral receptor well support this hypothesis, highlighting the conformational freedom of the aliphatic pending arm of **L1** and **L2** and the overall flexibility of both the ligands.

In all cases snapshot conformations evenly extracted from MD simulations range from elongated to compacted ones as provided by monitoring the distance separating the centroids (C_t) of the bpy or phen moieties. In particular, the C_t-C_t distance distribution (mean 9 Å; range 4-18Å) is very similar irrespective of the bpy *vs* phen moiety and the simulated media. Finally, the intramolecular H-bonds do not play a significant role in stabilizing the conformations of the ligands (in vacuum and in the simulated solvent). Summarizing the studied species do not show significant differences in terms of overall conformational flexibility, the only exception being the possible rotation at the 2',2' bond of bpy detected in the snapshot conformations extracted from the MD trajectories (Figure S27, ESI).

Table 2: Stability constants of the Cu^{2+}, Zn^{2+}, Cd^{2+} and Pb^{2+} complexes with **L1** and **L2**, determined in aqueous solution NMe_4Cl 0.1 M at 298 ± 0.1 K ([**L1**] = [**L2**] = 1 x 10^{-3} M). Values in parenthesis are standard deviations on the last significant figures

Equilibrium	Log K[a]			
	Cu^{2+}	Zn^{2+}	Cd^{2+}	Pb^{2+}
L1 + M^{2+} = $[M\mathbf{L1}]^{2+}$	21.8(1)	19.4(1)		
$[M\mathbf{L1}]^{2+}$ + H^+ = $[M(H\mathbf{L1})]^{3+}$	5.28(6)	5.04(3)		
$[M(H\mathbf{L1})]^{3+}$+ H^+ = $[M(H_2\mathbf{L1})]^{4+}$	3.48(6)	3.03(4)		
$[M\mathbf{L1}]^{2+}$ + OH^- = $[M\mathbf{L1}(OH)]^+$	3.8(1)	3.5(1)		
$[M\mathbf{L1}]^{2+}$ + M = $[M_2\mathbf{L1}]^{4+}$	8.3(1)	5.72(7)		
$[M_2\mathbf{L1}]^{4+}$ + H^+ = $[M_2(H\mathbf{L1})]^{5+}$	3.8(1)			
2**L1** + $3M^{2+}$ = $[M_3\mathbf{L1}_2]^{6+}$		49.7(1)		
$[M_2\mathbf{L1}]^{4+}$ + OH^- = $[M_2\mathbf{L1}(OH)]^{3+}$	6.5(1)	5.5(1)		
$[M_2\mathbf{L1}(OH)]^{3+}$ + OH^- = $[M_2\mathbf{L1}(OH)_2]^{2+}$	3.8(1)	4.5(1)		
L2 + M^{2+} = $[M\mathbf{L2}]^{2+}$	20.34(8)	16.8(1)	18.8(1)	16.4(1)
$[M\mathbf{L2}]^{2+}$ + H^+ = $[M(H\mathbf{L2})]^{3+}$	8.25(7)	6.8(1)	4.0(1)	4.4(1)
$[M(H\mathbf{L2})]^{3+}$+ H^+ = $[M(H_2\mathbf{L2})]^{4+}$	2.72(9)	3.4(1)	3.1(1)	3.3(1)
$[M\mathbf{L2}]^{2+}$ + OH^- = $[M\mathbf{L2}(OH)]^+$		4.4(1)	7.1(1)	7.8(1)
$[M\mathbf{L2}(OH)]^+$ + OH^- = $[M\mathbf{L2}(OH)_2]$			2.6(1)	3.5(1)
$[M\mathbf{L2}]^{2+}$ + $2OH^-$ = $[M\mathbf{L2}(OH)_2]$	7.31(7)			
$[M\mathbf{L2}]^{2+}$ + M^{2+} = $[M_2\mathbf{L2}]^{4+}$	9.25(7)	5.07(1)	4.8(1)	3.8(1)
$[M_2\mathbf{L2}]^{4+}$ + OH^- = $[M_2\mathbf{L2}(OH)]^{3+}$	6.25(7)			
$[M_2\mathbf{L2}(OH)]^{3+}$ + OH^- = $[M_2\mathbf{L2}(OH)_2]^{2+}$	5.26(7)			
$[M_2\mathbf{L2}]^{4+}$ + $2OH^-$ = $[M_2\mathbf{L2}(OH)_2]^{2+}$	11.51(4)	9.3(1)		

In polyamine ligands containing a phen or bpy moiety, including **L3** and **L4**, the heteroaromatic nitrogens are unequivocally coordinated to the metals.[8a-d,22-24,33] However, spectroscopic and/or X-ray diffraction data show that, in the case of first-row transition metals, such as Cu^{2+} or Zn^{2+}, this coordination mode precludes the simultaneous optimal interaction of the benzylic amine groups, adjacent to the metal-bound heterocyclic moiety, which results weakly bound or not bound to the metal.[8a,8b,8d,24,33,34]

For example, in the solid state structures of the Cu^{2+} and Ni^{2+} metal complexes of **L3** (GABBAN[34] and GABBER[34] refcodes in the Cambridge Structural Database version 5.40)[35] and the Cu^{2+}

complex of **L4**[8d] (XAMFEW refcode), the metal ion is bound by the heteroaromatic unit of the macrocycle, together with the three central amine functions. Only a single benzylic nitrogen is bound, although weakly, to the metal. In the [Zn**L3**]$^{2+}$ complex[24] (UBOKAX refcode) both the benzylic amine groups, adjacent to the metal-bound heterocyclic moiety, are not bound.

To ascertain the role of the two heteroaromatic moieties in metal binding in the mono- and dinuclear complexes with **L1** and **L2**, we recorded UV-vis spectra on solutions of ligands **L1** and **L2** in the presence of increasing amounts of the metals and the results for Zn^{2+} are reported in Figure 4 (see Figures S28-31 for the other metals, Supporting Information).

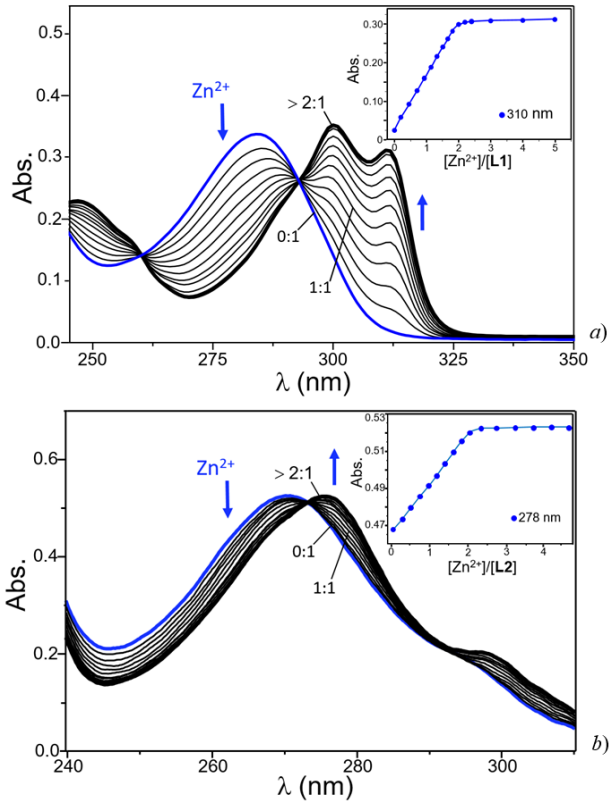

Figure 4: Absorption spectra of **L1** (a) and of **L2** (b) in the presence of increasing Zn^{2+} concentrations at pH 7. On top right of the figures are reported the variation of the absorbance at 310 nm and 278 nm, respectively for **L1** and **L2**, as a function of increasing metal ion amounts ([**L1**] = [**L2**] = 1x 10^{-5} M).

In fact, the absorption bands of bpy and phen are significantly affected by metal coordination. In particular, metal binding to bpy is accompanied by the disappearance of its original band at 290 nm and the simultaneous formation of a new structured band centered at ca 310 nm.[24] Analogously, metal coordination by phen generally results in a red-shift of its absorbtion band at 270 nm, often accompanied by slight changes in molar absorbance.[6e,7a,8a,8c] These spectral changes can be used as diagnostic tools to assess the involvement of the heteroaromatic moieties of ligands in metal binding.

As shown in Figure 4a for Zn^{2+}, ligand **L1** in the absence of metal ion features a band centered at 285 nm, as expected for the not-protonated form of the bpy moiety. Addition of increasing amounts of Zn^{2+} ion induces the disappearance of this absorption band, together with the progressive formation of a new structured band at *ca* 310 nm. In particular, the absorbance measured at 310 nm increases linearly up to 1.8:1 metal to ligand molar ratio (R), to achieve a constant value for molar ratios greater than 2.2, clearly indicating the formation of a stable dinuclear complex. Furthermore, the observed linear increase of absorbance of coordinated bpy, with no slope changes up to R = 1.8 suggests that each metal ion is coordinated, almost independently, by a single heteroaromatic unit in both mono- and dinuclear complexes.

Despite the absorption spectrum of phen is less affected by metal coordination with respect to bpy, Zn^{2+} binding by **L2** at neutral pH leads to a red-shift (*ca* 10 nm) of the typical UV band of phen at 268 nm, as shown in Figure 4b. As in the case of **L1**, the absorbance at 278 nm increases linearly up to R = 2 and then assumes a constant value, in agreement with the formation of stable 1:1 and 2:1 metal complexes, in which each Zn^{2+} ion is coordinated by a single phen unit. A similar behaviour is also observed in the case of the other metal cations (see Supporting Information, Figures S28-31).

Interestingly enough, the data in Table 2 point out that **L1** forms more stable mononuclear metal complexes than **L2**, the stability constants for its Cu^{2+} and Zn^{2+} complexes being 1.5 and 2.6 log. units higher than the corresponding **L2** complexes. The higher stability of the **L1** complexes with Cu^{2+} and Zn^{2+} cannot be ascribed to the binding ability of the different heteroaromatic units. In fact, phen is a better chelating agent than bpy[36,37] and, for instance, the stability constants of the $[Cu\mathbf{L}]^{2+}$ complex are 9.1 and 8.08 log unit with **L** = phen and bpy, respectively.[38] On the other hand, bpy is somewhat less rigid than phen, thanks to the possible rotation of the two heteroaromatic rings along the 2,2' axis (see also MD results). This feature, already observed in metal complexes with bpy-containing polyamine ligands,[23,24] would reinforce the overall interaction of **L1** with the metal guest, due to the reduced energetic cost, compared to **L2**, for ligand rearrangement to accomplish the stereochemical requirements of the metals. In contrast, the benzylic amine groups of **L1** and **L2** adjacent to the metal-bound heteroaromatic units are sterically hindered to interact with Cu^{2+} or Zn^{2+}, in particular in the case of **L2**, which contains a more rigid phen moiety. On the other hand, bpy has a more marked electron poor nature than phen and exerts a higher electron-withdrawing effect on lateral side arms. In particular the 6 and 6' carbons of bpy are known to be much more electron poor than the 2 and 9 carbons of phen.[39,40] As a result, the benzylic amine groups N1 and N1' (see Scheme 1 for atom labelling) in **L1** result poorer σ-donors that the corresponding amine functions of **L2.**

The latter characteristic seems to play a minor role in determining the stability of the complexes. However, the benzylic nitrogens are less involved or even not involved in Cu^{2+} or Zn^{2+} coordination by **L1** and **L2**, as already observed in other phen- or bpy- containing polyamine ligands, including **L3** and **L4**.[8a,8b,8d,24,33,34] This applies in particular, to the metal complexes with the bpy-containing ligand **L3**, in which the benzylic amine groups are also poorer σ-donors and, actually, the crystal structure of the $[Zn\mathbf{L3}]^{2+}$ complex shows that the benzylic amine groups are not bound to the metal.[24]

As often found for complexes containing weakly bound or not bound amine groups, both the Cu^{2+} and Zn^{2+} complexes with **L1** and **L2** affords mono- and di-protonated species, likely due to protonation of the amine groups in benzylic position, poorly involved in metal coordination. Interestingly enough, the protonation constants of the complexes with **L1** are lower than those of the corresponding complexes with **L2**, in agreement with lower σ-donor ability of the benzylic amine groups of **L1**.

Both the mononuclear $[M\mathbf{L1}]^{2+}$ and $[M\mathbf{L2}]^{2+}$ complexes (M = Cu^{2+} and Zn^{2+} in the case of **L1**, M = Cu^{2+}, Zn^{2+}, Cd^{2+} and Pb^{2+} for **L2**), can also add a second metal to form a binuclear $[M_2\mathbf{L}]^{4+}$ species. However, the constant for the addition of a second metal ion to the $[M\mathbf{L}]^{2+}$ is dramatically lower than that found for the formation of the mononuclear complexes. This can be attributed not only to the electrostatic repulsion between the two metal cations, kept at close distance by the ligand frameworks, but also to the energetic cost for polyamine chain reorganization upon coordination of the second metal.

The present data are not sufficient to infer hypothesis on the coordination environment of the metals in the dinuclear complexes, although the UV-vis spectrophotometric titrations strongly suggest that each metal in the $[M_2\mathbf{L}]^{4+}$ complex is bound by a single heteroaromatic moiety.

Fluorimetric response of L1 and L2 to metal coordination. The fluorescence emission characteristics of **L1** and **L2** were investigated by means of spectrofluorimetric measurements on the ligands in the presence of each selected metal ion in 1:1 and 1:2 molar ratios at different pH values or at fixed pH values in the presence of increasing amount of the metal.

In the case of **L1**, Cu^{2+} or Zn^{2+} coordination induces a marked quenching of the emission, as shown in Figures 5a,b (Zn^{2+}) and S32 (Cu^{2+}) for solutions containing ligand and metal in 1:1 molar ratio, In fact, the systems are almost non-emissive all over the pH region in which the metal complexes are present in solution. A renewal of the fluorescence emission is observed only at acidic pH values (below pH 4 in the case of Zn^{2+}, Figure 5b), with the formation of the typical band of the

bipyridinium ion at 345 nm. The emission is mainly due to metal decomplexation and consequent formation in solution of emissive protonated species of the ligand ($[H_6\mathbf{L1}]^{6+}$ and $[H_7\mathbf{L1}]^{7+}$), in which the heteroaromatic unit is protonated.

A different behaviour is observed in the case of **L2** in the presence of 1 equiv. of Zn^{2+}. In fact, the system results emissive in a wide pH range. Figure 5c shows that in the range of pH within 4-8 the broad band of the phen fluorophore, displaying a maximum at 395 nm and a marked shoulder at 375 nm, appears in the spectra, the maximum fluorescence emission being observed at pH 5.5.

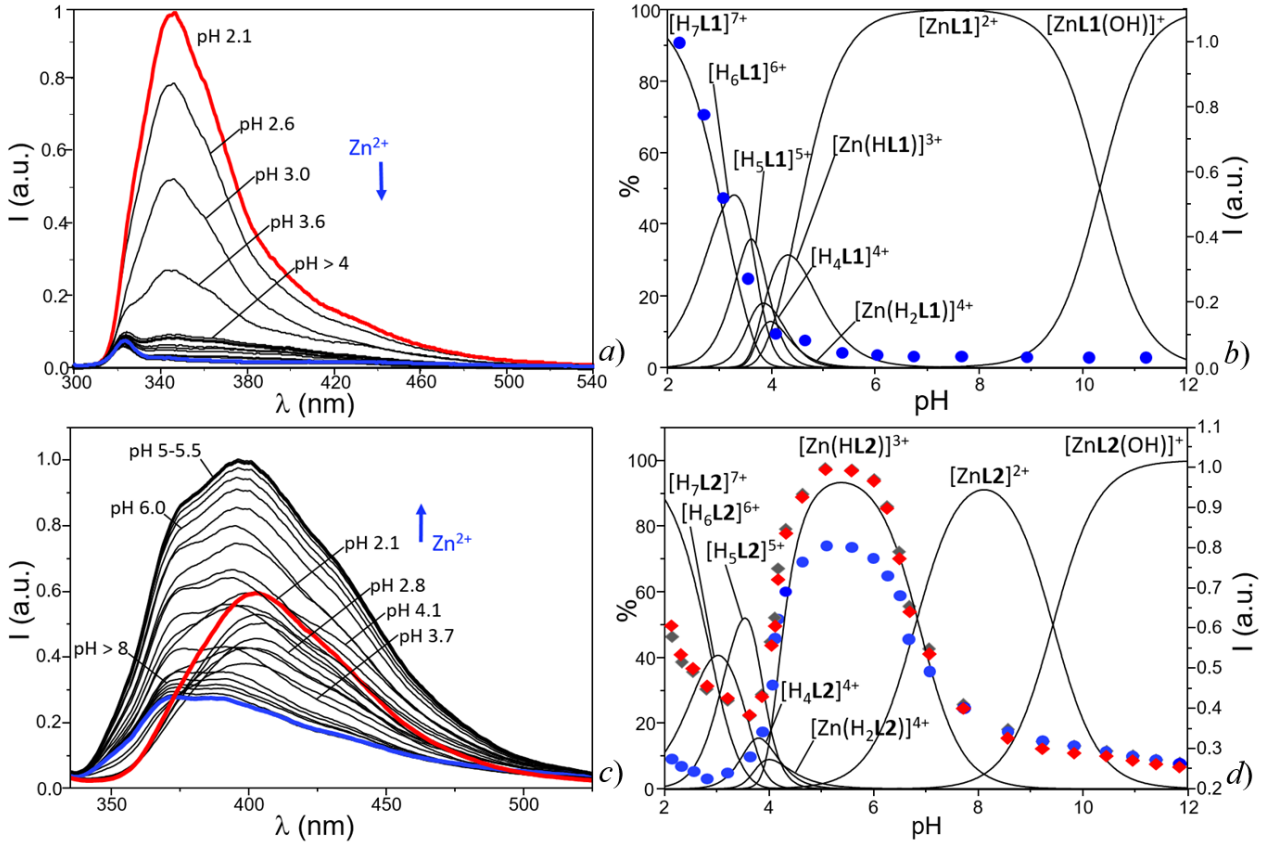

Figure 5: Fluorescence emission spectra collected for the systems L:Zn^{2+} 1:1 at different pH values; L = **L1** (a), L = **L2** (c). On the right-side of figures are reported the correspondent variation of emission at 345 nm (blue circles) for **L1** (b) and at 375 nm (blue circles), 395 nm (grey squares) and 403 nm (red squares) for **L2** (d) overlapped with the relative distribution diagrams of the species present in solution ([**L1**] = [**L2**] = 1x 10^{-5} M, λ_{exc} = 290 nm).

Above pH 8, the ligand is basically quenched (Figures 5c,d), while at lower pH values the spectra are characterized by the disappearance of the phen emission band and the appearance of the typical red-shifted band of phenanthrolinium, centered at 403 nm. Superimposition of the emission monitored at 375, 395 and 403 nm with the distribution diagram of the species formed in solution containing **L2** and Zn^{2+} in 1:1 molar ratio points out that the observed emission of phen (pH 4-8) is likely due to the formation of the monoprotonated complex $[Zn(H\mathbf{L2})]^{3+}$. On the other hand, similarly to **L1**, the appearance of the phenanthrolium ion band is due to metal decomplexation and

consequent formation of ligand protonated species ($[H_6\mathbf{L2}]^{6+}$ and $[H_7\mathbf{L2}]^{7+}$), in which phen is protonated. Interestingly enough, the $[Zn\mathbf{L2}]^{2+}$ and $[Zn\mathbf{L2}(OH)]^{+}$ complexes result basically non-emissive.

Despite the fluorescence emission displayed by the Zn^{2+} complexes with bpy and phen in aqueous solution, the mononuclear complexes with **L1** and **L2** are basically not emissive, with the only exception of the protonated $[Zn(H\mathbf{L2})]^{3+}$ complex. The non emissive nature of the Zn^{2+} complexes appears a common feature of polyamine ligands incorporating a phen or bpy units within their backbone, including **L3** and **L4**,[8a,8c,22-24] and has been usually attributed to photoinduced electron transfer (PET) process from a not Zn^{2+}-coordinated amine group to the excited fluorophore. This could also apply to the present complexes, which display a benzylic amine group (N1), nicely placed closed to the fluorogenic unit, whose electron pair is available to give a PET process to the adjacent fluorophore in its excited state. Protonation of this amine group would inhibit the quenching effect, as actually observed in the $[Zn(H\mathbf{L2})]^{3+}$ species. In principle, the fluorescence of the $[Zn(H\mathbf{L2})]^{3+}$ complex could be attributed to proton localization either on the N1' nitrogen atom adjacent to the Zn^{2+}-bound phen or on the benzylic nitrogen N1 close to the second fluorophore not involved in metal coordination. Actually, the latter hypothesis would lead to a better minimization of the electrostatic repulsion between the metal cation and the ammonium group of $[Zn(H\mathbf{L2})]^{3+}$. At the same time, the emission band observed for the $[Zn(H\mathbf{L2})]^{3+}$ complex is ca. 10 nm red-shifted with respect to that observed for free phen, leading us to suggest that the fluorescence emission arises from a phen unit partially involved in proton binding, probably thanks to hydrogen bonding with the adjacent ammonium groups in benzylic position. These considerations suggest that protonation occurs on the N1 aliphatic nitrogen adjacent to the phen moiety not involved in metal binding, as sketched in Scheme 3. As a result, in this system the two equal phen units actually play different roles. While the first one is used for Zn^{2+} binding, the second one acts as signalling moiety.

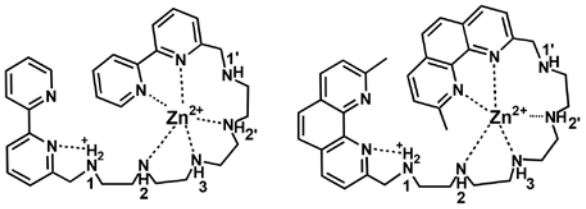

Scheme 3: Sketch of the proposed coordination model for the specie $[Zn(H\mathbf{L1})]^{3+}$ (left) and $[Zn(H\mathbf{L2})]^{3+}$ (right) respectively.

On the other hand, in the case of **L1**, only a very weak emission is observed in the pH range 4-6, in which the monoprotonated species $[Zn(H\mathbf{L1})]^{3+}$ is formed. This different behaviour can be

reasonably ascribed to the lower proton binding affinity of **L1,** which results in a much lower percentage of protonated complexed species present in solution, coupled with the lower intensity of emission normally observed for bpy with respect to phen.

We also analyzed the fluorescence of **L2** in the presence of the four selected metal cations at neutral pH, in order to compare the emission properties of their complexes.

As shown in Figure 6, addition of increasing amounts of Zn^{2+} induces a linear increase of the emission of phen up to a metal to ligand 1:1 molar ratio (R), accompanied by a red-shift of the band. Further increase of metal ion causes a linear decrease of the emission as R increases from 1 to 2. This data is in agreement with the successive formation of a 1:1 and 2:1 metal-ligand complex. The emission intensity further decreases for R > 2, to finally assumes a constant value for R > 4.

In the dinuclear Zn^{2+} complex $[Zn_2\mathbf{L2}]^{4+}$, the benzylic nitrogens are likely not coordinated to the metals and, therefore, they can enable a PET process which quenches the phen emission. At the same time, the dinuclear $[Zn_2\mathbf{L2}]^{4+}$ complex does not protonate in solution (see Table 2), preventing any inhibiting effect of the PET process. Therefore, the **L2** emission is controlled not only by pH, but also by metal concentration, In fact, while simultaneous binding of a single Zn^{2+} cation and H^+ switches on the phen emission, binding of a second metal brings back the system to its OFF state.

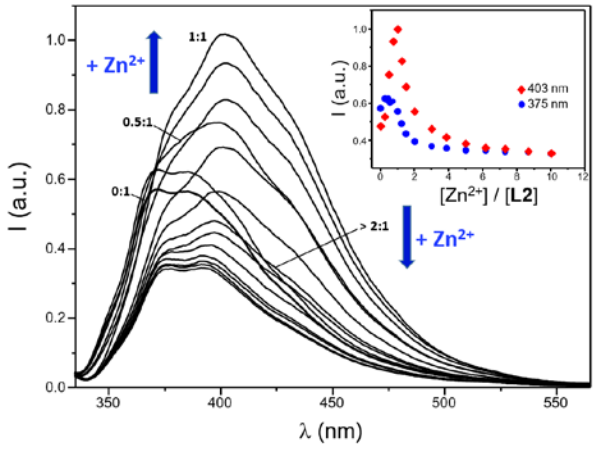

Figure 6: Fluorescence emission spectra of **L2** at pH 5.5 in the presence of increasing Zn^{2+} concentrations. On top right of the figure is shown the variation of emission at 375 and 403 nm, as a function of the $[Zn^{2+}]/[\mathbf{L2}]$ molar ratio ($[\mathbf{L2}] = 1 \times 10^{-5}$ M, $\lambda_{exc} = 290$ nm).

Differently from Zn^{2+}, Cd^{2+} complexation at pH 7 is accompanied by a slight reduction of the fluorescence emission of **L2** (see Figures S33 a-b, ESI). In particular, as shown in Figures S34 a-b (ESI), addition of increasing amounts of Cd^{2+} to a solution of **L2** determines a linear decrease of its fluorescence intensity (in this condition the emission intensity is 45% reduced) accompanied by a

red-shift emission. A further decrease of the emission is observed for R > 1, due to the formation of dinuclear complexes. Similarly to Cd^{2+}, Cu^{2+} and Pb^{2+} complexation leads to emission quenching (see ESI, figures S33-34). While the quenching effect observed in the case of Cd^{2+} and Pb^{2+} can be related to their heavy nature, the emission decrease induced by Cu^{2+} is likely due to its paramagnetism. The fluorescence emission intensity of the ligand in the presence of the same amount (1 equiv.) of the 4 metals is compared in Figure 7.

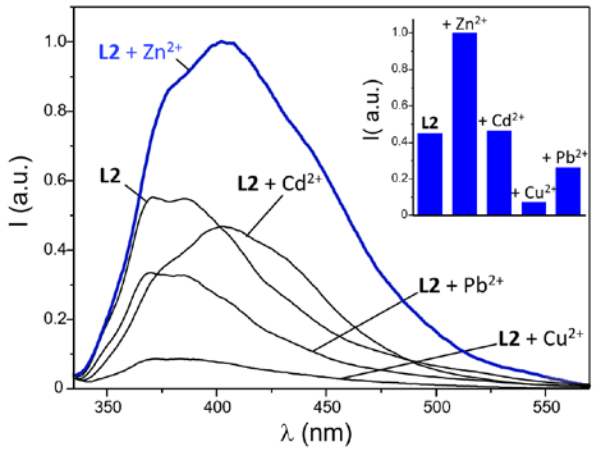

Figure 7: Emission spectra of an aqueous solution of **L2** in the presence of 1 eq. of Zn^{2+}, Cd^{2+}, Cu^{2+} and Pb^{2+}. On top right of the figure is reported the relative fluorescence emission of **L2** at 403 nm in the absence and in the presence of 1 eq. of Zn^{2+}, Cd^{2+}, Cu^{2+} and Pb^{2+} ([**L1**] = [**L2**] = 1 x 10^{-5} M, pH = 7, λ_{exc} = 290 nm).

Concluding remark.

This paper shows that small structural differences can strongly affect the binding and sensing properties toward selected metals. Despite the lower thermodynamic stability of the Cu^{2+} and Zn^{2+} complexes with bpy than those with phen, **L1** forms slightly more stable complexes with these metals, thanks to the possible rotation along the 2,2' bond of bpy, allowing to better accomplish the metal stereochemical requirements. In the complexes with both **L1** and **L2**, the benzylic amine groups are sterically hindered to bind metal cations. However, these nitrogens differ in phen and bpy in their σ-donor properties. In fact, bpy is more electron poor than phen, in particular on the 6 and 6' carbons, and exerts a greater electron-withdrawing effect on the benzylic amine groups, which are less basic than in **L2**. While this characteristic does not seem to affect the stability of the complexes, it strongly influences the emission of the Zn^{2+} complexes. The [Zn**L2**]$^{2+}$ complex is basically not emissive, due to a PET process from the lone pair of the benzylic nitrogens to the excited phen unit. Protonation of these amine groups, with the formation of protonated complexes, inhibits the PET process and switches ON the emission of phen over a wide pH range, including neutral pH. In contrast, the poor propension of the **L1** benzylic nitrogens to bind acidic protons

leads to the formation of low percentages of $[ZnH\mathbf{L1}]^{3+}$ or $[ZnH_2\mathbf{L1}]^{4+}$ and the system maintains its OFF state. As a result of the structural/electronic characteristics of **L2**, this ligand results a peculiar molecular switch whose emission is modulated by both metal and proton binding. In fact, binding of a single metal maintains the system in its non-emissive state. Only simultaneous binding of a single metal and acidic protons switches on the emission, which is, in turn, quenched again in the presence of a second Zn^{2+} cation.

EXPERIMENTAL SECTION

Synthesis of 1,15-*bis*-[6-(2,2'-bipyridyl)]-2,5,8,11,14-pentatosyl-2,5,8,11,14-pentaaza-octadecane (3). A solution of 6-(bromomethyl)-2,2'-bipyridine (**1,** 992 mg, 4 mmol) in dry acetonitrile (100 ml) was added, under a nitrogen atmosphere, to a boiling stirred suspension of the tosylated polyamine **2** (2.594 g, 2 mmol) and K_2CO_3 (2.76 g, 20 mmol) in dry acetonitrile (100 ml) over a period of 1 h. The mixture was kept at reflux under stirring for additional 2 h. The suspension was filtered on Celite, washed with acetonitrile, and the resulting solution was evaporated to obtain a crude yellowish solid, which was purified by column cromatography on neutral alumina, using petroleum ether/ethyl acetate 1:1 as eluent. The resulting solution was vacuum evaporated and dried in vacuum to afford pure compound **3** as a colourless solid (855 mg, 33% yield).

El. An. Calcd for $C_{65}H_{69}N_9S_5O_{10}$: C, 60.11 %; H, 5.51 %; N, 9.71 %. Found: C, 60.02 %; H, 5.59 %; N, 9.64 %

^{1}H-NMR ($CDCl_3$, 400 MHz): δ(ppm) 8.70 (d, 2H), 8.58 (m, 4H), 8.21 (m, 2H), 8.01 (m, 2H), 7.89 (m, 2H), 7.70 (m, 10H), 7.31 (m, 10H), 4.23 (s, 4H), 3.36 (m, 8H), 3.19 (m, 8H), 2.45 (s, 3H), 2.43 (s, 6H), 2.40 (s, 6H).

Synthesis of 1,15-*bis*-[6-(2,2'-bipyridyl)]-2,5,8,11,14-pentaazaoctadecane (L1). Compound **3** (0.5 mmol, 8 mg) and phenol (25 mmol, 2.35 g) were dissolved in HBr/AcOH 33% (50 ml). The reaction mixture was kept under stirring at reflux (ca. 90° C) for 20 hours, until the formation of a yellowish solid resulted. 100 ml of dichloromethane were added to complete the precipitation and the mixture was stirred for additional 1 hour. The solid was filtered and washed with dichloromethane to remove the residual phenol. Ligand **L1**, as dihydrated penthydrobromide salt (**L1**·5HBr·2H_2O), was recrystallized from a EtOH:water 20:1 (v/v) mixture, affording a colourless solid which was filtered off and dried in vacuum (358 mg, 74 % yield).

El. An. Calcd for $C_{30}H_{50}N_9O_2Br_5$: C, 37.21 %; H, 5.20 %; N, 13.01 % Found: C, 37.02 %; H, 5.32 %; N, 12.95 %.

^{1}H-NMR (D_2O, pD = 1.5, 400 MHz): δ(ppm) 8.95 (d, 2H), 8.78 (m, 4H), 8.41 (m, 2H), 8.24 (m, 2H), 8.16 (m, 2H), 7.78 (m, 2H), 4.75 (s, 4H); 3.74 (m, 8H), 3.60 (m, 8H). ^{13}C-NMR (D_2O, pD =1.5) δ(ppm) 152.5,148.5, 148.0, 146.4, 142.4, 141.1, 128.1, 126.7, 125.2, 123.4, 51.6, 44.7, 44.4, 44.2, 43.7. ESI mass spectrum: 526.34 (Z =1, $[M + H]^+$), 548.32 (Z =1, $[M + Na]^+$)

Synthesis of 1,15-*bis*-[2-(1,10-phenanthroline)-9-methyl]-2,5,8,11,14-pentatosyl-2,5,8,11,14-pentaazaoctadecane (5). Compound **5** was obtained from **4** (971 mg, 4 mmol) and **2** (2.594 g, 2 mmol) by using a similar procedure to that reported for **3**. In this case, the addition of the solution in CH_3CN of **4** to the CH_3CN solution of **2** was performed in 5 h and then the resulting suspension was kept at reflux under stirring for 12 h (660 mg, 24 % yield).

El. An. Calcd for $C_{71}H_{75}N_9S_5O_{10}$: C, 62.03 %; H, 5.50 %; N, 9.17 %. Found: C, 62.20 %; H, 5.45 %; N, 9.22 %

^{1}H-NMR ($CDCl_3$, 400 MHz): δ(ppm) 8.98 (d, 2H), 8.37 (d, 2H), 7.99 (m, 6H), 7.79 (d, 2H), 7.69 (m, 10H), 7.32 (m, 10H), 4.63 (s, 4H), 3.49 (m, 8H), 3.27 (m, 8H), 2.89 (s, 6H), 2.47 (s, 3H), 2.41 (s, 6H), 2.37 (s, 6H).

Synthesis of 1,15-*bis*-[2-(1,10-phenanthroline)-9-methyl]-2,5,8,11,14-pentaazaoctadecane (L2)

L2 was obtained from **5** (687 mg, 0.5 mmol) by using the same procedure reported for **L1**. The ligand was obtained as colorless pentahydrobromide salt (**L2**·5HBr, 347 mg, 69 % yield)

El. An. Calcd for $C_{36}H_{50}N_9Br_5$: C, 42.88 %; H, 5.00 %; N, 12.50 %. Found: C, 42.69 %; H, 5.09 %; N, 12.43 %.

^{1}H-NMR (D_2O, pD = 1.5, 400 MHz: δ(ppm) 9.11 (d, 2H), 8.71 (d, 2H), 8.21 (m, 6H), 8.00 (d, 2H), 4.97 (s, 4H), 3.83 (m, 8H), 3.63 (m, 8H), 3.23 (s, 6H). ^{13}C-NMR (D_2O, pD = 1.5): δ(ppm): 157.70, 152.9, 147.13, 139.73, 137.86, 136.33, 130.22, 129.55, 128.80, 127.28, 126.45, 125.02, 52.04, 44.81, 44.52, 44.23, 43.76, 21.28. ESI mass spectrum: 301.68 (Z =2, $[M + 2H]^{2+}$), 602.37 (Z =1, $[M + H]^+$), 624.35 (Z =1, $[M + Na]^+$)

Potentiometric measurements. Equilibrium constants for protonation and metal ion binding of ligands were determined by pH-metric measurements in degassed 0.1M NaCl at 298 ± 0.1 K, by using equipment and procedures which have been already described.[41,42]

An Ag/AgCl electrode in saturated KCl solution was used as reference electrode, while the glass electrode was calibrated as a hydrogen concentration probe by titrating known amounts of HCl with CO_2-free NaOH solutions. The equivalent point, the standard potential E^o and the ionic product of water (pK_w = 13.73 ± 0.01 at 298.1 K in 0.1 M NaCl) were determined by using the Gran's method.[43] Three titration experiments (consisting of 100 data points for each one) were performed in the pH range 2-11. 1 x 10^{-3} mol/dm^3 ligand concentrations were employed in the potentiometric measurements. In metal ion titrations the metal concentration was varied from 0.8[L] to 1.8[L] (L = **L1** or **L2**). The computer program HYPERQUAD[44] was used to determine the protonation constants of ligands together with their metal ion binding constants from e.m.f. data. Distribution diagrams were obtained by using the Hyss program.[45]

NMR mesurements. NMR experiments were carried out by using on a Bruker Avance 400 MHz instrument by using method and procedure which has been already described.[46] The pH was calculated from the measured pD value by using the relationship pH = pD – 0.40.[47]

Electronic absorption and fluorescence measurements. Absorption and fluorescence spectra were registered on a Perkin-Elmer Lambda 6 spectrophotometer and on a Perkin-Elmer LS55 spectrofluorimeter, respectively. An excitation wavelength of 290 nm was used to record fluorescence spectra of both ligands. All measurements were performed at 298.0 ± 0.1 K.

Molecular Modeling Procedures. The starting geometries for **L1** and **L2**, were derived from the solid state structure of the closely related ligands reported in literature.[48,49] Molecular dynamics (MD) simulations were performed both in vacuum and in implicit solvent, the latter simulated by using a distance dependent dielectric constant set to 80r (T=300K, time step = 1fs, equilibration time = 100ps, production time = 1000ps), then 100 snapshot conformations were extracted from each MD trajectory. The programs used for the energy minimization and MD were the simulation protocols Minimization, Standard Dynamics Cascade and Analyse Trajectory, implemented in Accelrys Discovery Studio 2.1.[50] The Force Field used for all the simulations was CHARMm.[51] Further details on the experimental procedures are given within the Supporting Information.

Acknowledgment. Financial support from MIUR (PRIN 2017 project 2017EKCS35) is gratefully acknowledged. A.B. thank 'Fondazione Cassa di Risparmio di Firenze' for financial support.

REFERENCES

1- a) D. Wu, A. C. Sedgwick, T. Gunnlaugsson, E. U. Akkaya, J. Yoon and T. D. James, *Chem. Soc. Rev.* **2017**, 46, 7105-7123. b) V. Amendola, M. Bonizzoni, D. Esteban-Gómez, L. Fabbrizzi, M. Licchelli, F. Sancenón and A. Taglietti, *Coord. Chem. Rev.* **2006**, 250, 1451-1470. c) V. Balzani, G. Bergamini and P. Ceroni, *Coord. Chem. Rev.* **2008**, 252, 2456-2469. d) B. Valeur and I. Leray, *Coord. Chem. Rev.* **2000**, 205, 3-40. e) A. Bianchi, E. Delgado-Pinar, E. Garcia-Espana, C. Giorgi, F. Pina, *Coord Chem Rev.* **2014**, 260, 156-215.

2- a) M. Formica, V. Fusi, L. Giorgi, M. Micheloni *Coord. Chem. Rev.* **2012**, 256, 170-192. b) C. Lodeiro, J. L. Capelo, J. C. Mejuto, E. Oliveira, H. M. Santos, B. Pedras, C. Nuñez *Chem. Soc. Rev.* **2010**, 39, 2948-2976. c) B. Kaur, N. Kaur, S. Kumar *Coord. Chem. Rev.* **2018**, 358, 13-69. d) G. Sivaraman, M. Iniya, T. Anand, N. G. Kotla, O. Sunnapu, S. Singaravadivel, A. Gulyani, D. Chellappa *Coord. Chem. Rev.* **2018**, 357, 50-104. e) H. Lee, K.-I. Hong, W.-D. Jang, *Coord. Chem. Rev.* **2018**, 354, 46-73.

3- a) C. Caltagirone, P. A. Gale, *Chem. Soc. Rev.* **2009**, **38**, 520-563. ~~b) P. R. Sahoo, K. Prakash, S. Kumar, S. *Coord. Chem. Rev.* **2018**, 357, 18-49~~. b) Y. Ding, W.-H. Zhu, Y. Xie, *Chem. Rev.* **2017**, 117, 2203-2256. c) J. A. Cotruvo Jr., A. T. Aron, K. M. Ramos-Torres, M. Karla C. J. Chang, *Chem. Soc. Rev.* **2015**, 44, 4400-4414. ~~e) Y. Ding, Yubin, Y. Tang, W. Zhu, Y. Xie, *Chem. Soc. Rev.* **2015**, 44, 1101-1112.~~

4- a) X. Qian, Z. Xu, *Chem. Soc. Rev.* **2015**, 44, 4487-4493. b) C. Lodeiro, F. Pina, *Coord. Chem. Rev*. **2009**, 253, 1353-1383. c) ~~S. Singha, Y. W. Jun, S. Sarkar, K. H. Ahn *Acc. Chem. Res.* **2019**, 52, 2571-2581~~. b) T. Joshi, B. Graham, L. Spiccia, *Acc. Chem. Res.* **2015**, 48, 2366-2379. e) ~~S. K. Kim, D. H. Lee, J. Hong, J. Yoon, *J. Acc. Chem. Res.* **2009**, 42, 23-31.~~

5- a) V. Amendola, G. Bergamaschi, A. Miljkovic, *Supramol. Chem.* **2018**, 30, 236-242. b) N. Kwon, Y. Hu, J. Yoon**,** *ACS Omega* **2018**, 3, 13731-13751. c) C. M. Ackerman, S. Lee, C. J. Chang, *Anal. Chem.* **2017**, 89, 22-41. d) M. C. Aragoni, M. Arca, A. Bencini, C. Caltagirone, L. Conti, A. Garau, B. Valtancoli, F. Isaia, V. Lippolis, F. Palomba, L. Prodi, N. Zaccheroni, *Supramol. Chem.* **2017**, 29, 912-921. e) D. W. Domaille, E. L. Que, C. Chang, *J. Nat. Chem. Biol*. **2008**, 4, 168-175.

6- a) Y. Fan, Y. F. Long, Y. F. Li, *Anal. Chim. Acta* **2009**, 653, 207-211. b) P. Pallavicini, L. Pasotti, S. Patroni, *Dalton Trans.* **2007**, 5670-5677. c) R. Gavara, J. Mateos, F. Sabaté, R. Belda, J. M. Llinares, E. García-España, L Rodríguez, *Eur. J. Inorg. Chem.* **2018**, 4550-4555. d) A. Garau, A. Bencini, A. J. Blake, C. Caltagirone, L. Conti, F. Isaia, V. Lippolis, R. Montis, P. Mariani, M. A. Scorciapino, *Dalton Trans.* **2019**, 48, 4949-4960. e) J. Pitarch, M. P. Clares, R. Belda, R. D. Costa, P. Navarro, E. Orti, C. Soriano, E. Garcia-España, *Dalton Trans*. **2010**, 39, 7741-7746.

7- a) D. Wu, L. Chen, W. Lee, G. Ko, J. Yin and J. Yoon, *Coord. Chem. Rev.* **2018**, 354, 74-97. b) A. P. De Silva, H. Q. N. Gunaratne, T. Gunnlaugsson, A. J. M. Huxley, C. P. McCoy, J. T. Rademacher and T. E. Rice, *Chem. Rev.* 97, **1997**, 1515-1566. c) V. Amendola, L. Fabbrizzi, F. Foti, M. Licchelli, C. Mangano, P. Pallavicini, A. Poggi, D. Sacchi, A. Taglietti, Sacchi and A. Taglietti, *Coord. Chem. Rev.* **2006**, 250, 273-299. d) L. Prodi, F. Bolletta, M. Montalti and N. Zaccheroni, *Coord. Chem. Rev.* **2000**, 205, 59-83. e) ~~L. E. S. Figueroa, M. E. Moragues, E. Climent, A. Agostini, R. Martínez-Máñez and F. Sancenón, *Chem. Soc. Rev.* **2013**, 42, 3489-3613.~~ f) R. Martínez-Máñez and F. Sancenón, *Chem. Rev.* **2003**, 103, 4419-4476. ~~g) M. D. Best, S. L. Tobey and E. V. Anslyn, *Coord. Chem. Rev.* **2003**, 240, 3-15. h)~~ g) N. Busschaert, C. Caltagirone, W. Van Rossom and P. A. Gale, *Chem. Rev.* **2015**, 115, 8038-8155.

8- a) A. Bencini, M. A. Bernardo, A. Bianchi, V. Fusi, C. Giorgi, F. Pina and B. Valtancoli,

Eur. J. Inorg. Chem. **1999**, 11, 1911-1918. b) C. Bazzicalupi, A. Bencini, A. Bianchi, C. Giorgi, V. Fusi, B. Valtancoli, M. A. Bernardo and F. Pina, *Inorg. Chem.* **1999**, 38, 3806-3813. c) C. Bazzicalupi, A. Bencini, S. Biagini, A. Bianchi, E. Faggi, C. Giorgi, M. Marchetta, F. Totti and B. Valtancoli, *Chem. - A Eur. J.* **2009**, 15, 8049-8063. d) D. K. Chand, H. J. Schneider, A. Bencini, A. Bianchi, C. Giorgi, S. Ciattini and B. Valtancoli, *Chem. - A Eur. J.* **2000**, 6, 4001-4008. e) P. D. Beer and P. A. Gale, *Angew. Chemie - Int. Ed.* **2001**, 40, 486-516. f) C. Bazzicalupi, A. Bencini, Bonaccini, C. Giorgi, P. Gratteri, S. Moro, M. Palumbo, A. Simionato, J. Sgrignani, C. Sissi, C., *Inorg. Chem.* **2008**, 47, 5473-5484.

9- a) F. Pina, M. A. Bernardo and E. García-España, *Eur. J. Inorg. Chem.* **2000**, 2143-2157. ~~b) J. W. Steed, in *Encyclopedia of Supramolecular Chemistry*, **2004**, pp. 1401-1411.~~ b) M. Carla Aragoni, M. Arca, A. Bencini, A. J. Blake, C. Caltagirone, A. Decortes, F. Demartin, F. A. Devillanova, E. Faggi, L. S. Dolci, A. Garau, F. Isaia, V. Lippolis, L. Prodi, C. Wilson, B. Valtancoli and N. Zaccheroni, *Dalton Trans.* **2005**, 2994-3004. c) R. Parkesh, T. C. Lee and T. Gunnlaugsson, *Org. Biomol. Chem.* **2007**, 5, 310-317.

10- ~~a) M. Soibinet, V. Souchon, I. Leray and B. Valeur, *J. Fluoresc.* **2008**, 18, 1077-1082. b) V. Souchon, I. Leray and B. Valeur, *Chem. Commun.* **2006**, 4224-4226. c) P. Pallavicini, Y. A. Diaz-Fernandez, F. Foti, C. Mangano and S. Patroni, *Chem. - A Eur. J.* **2007**, 13, 178-187.~~ a) G. Ambrosi, C. Battelli, M. Formica, V. Fusi, L. Giorgi, E. Macedi, M. Micheloni, R. Pontellini, L. Prodi, *New J. Chem.* **2009**, 33, 171-180.

11- L. Conti, A. Bencini, C. Ferrante, C. Gellini, P. Paoli, M. Parri, G. Pietraperzia, B. Valtancoli, C. Giorgi, *Chem. Eur. J.* **2019**, 25, 10606-10615.

12- a) K. P. Carter, A. M. Young and A. E. Palmer, *Chem. Rev.* **2014**, 114, 4564-4601. b) ~~S. Lee, K. K. Y. Yuen, K. A. Jolliffe and J. Yoon, *Chem. Soc. Rev.* **2015**, 44, 1749-1762~~. b) Z. Xu, J. Yoon and D. R. Spring, *Chem. Soc. Rev.* **2010**, 39, 1996-2006. c) F. Bartoli, A. Bencini, L. Conti, C. Giorgi, B. Valtancoli, P. Paoli, P. Rossi, N. Le Bris and R. Tripier, *Org. Biomol. Chem.* **2016**, 14, 8309-8321.

13- S. Amatori, G. Ambrosi, E. Borgogelli, M. Fanelli, M. Formica, V. Fusi, L. Giorgi, E. Macedi, M. Micheloni, P. Paoli, P. Rossi and A. Tassoni, *Inorg. Chem.* **2014**, 53, 4560-4569.

14- C. Bazzicalupi, A. Bencini, A. Bianchi, L. Borsari, A. Danesi, C. Giorgi, C. Lodeiro, P. Mariani, F. Pina, S. Santarelli, A. Tamayo and B. Valtancoli, *Dalton Trans.* **2006**, 4000-4010.

15- C. Bazzicalupi, A. Bencini, S. Ciattini, F. Denat, P. Désogère, C. Goze, I. Matera and B. Valtancoli, *Dalton Trans.* **2010**, 39, 11643-11653.

16- J. Alarcón, M. T. Albelda, R. Belda, M. P. Clares, E. Delgado-Pinar, J. C. Frías, E. García-España, J. González and C. Soriano, *Dalton Trans.* **2008**, 6530-6538.

17- M. Boiocchi, L. Fabbrizzi, M. Licchelli, D. Sacchi, M. Vázquez and C. Zampa, *Chem. Commun.* **2003**, 3, 1812-1813.

18- M. C. Aragoni, M. Arca, A. Bencini, A. J. Blake, C. Caltagirone, G. De Filippo, F. A. Devillanova, A. Garau, T. Gelbrich, M. B. Hursthouse, F. Isaia, V. Lippolis, M. Mameli, P. Mariani, B. Valtancoli and C. Wilson, *Inorg. Chem.* **2007**, 46, 4548-4559.

19- M. Chadlaoui, B. Abarca, R. Ballesteros, C. R. De Arellano, J. Aguilar, R. Aucejo and E. García-España, *J. Org. Chem.* **2006**, 71, 9030-9034.

20- L. Fabbrizzi, M. Licchelli, F. Mancin, M. Pizzeghello, G. Rabaioli, A. Taglietti, P. Tecilla and U. Tonellato, *Chem. - A Eur. J.* **2002**, 8, 94-101.

21- A. Bencini, B. Valtancoli, L. Conti, I. Palchetti, D. Voccia, F. Bettazzi and C. Giorgi, *Eur. J. Inorg. Chem.* **2018**, 2675-2679.

22- C. Bazzicalupi, A. Bencini, V. Fusi, C. Giorgi, P. Paoletti and B. Valtancoli, *J. Chem. Soc. Dalton Trans.* **1999**, 393–400.

23- P. Arranz, C. Bazzicalupi, A. Bencini, A. Bianchi, S. Ciattini, P. Fornasari, C. Giorgi and B. Valtancoli, *Inorg. Chem.* **2001**, 40, 6383-6389.

24- C. Lodeiro, A. J. Parola, F. Pina, C. Bazzicalupi, A. Bencini, A. Bianchi, C. Giorgi, A.

Masotti and B. Valtancoli, *Inorg. Chem.* **2001**, 40, 2968-2975.
25- G. R. Newkome, V. K. Gupta and F. R. Fronczek, *Inorg. Chem.* **1983**, 22, 171-174.
26- A. Bencini, A. Bianchi, M. Micheloni, P. Orioli, P. Paoletti, E. Garcia-España and S. Mangani, *Inorg. Chem.* **1988**, 27, 1104-1107.
27- G. R. Newkome, K. J. Theriot, V. K. Gupta, F. R. Fronezek and G. R. Baker, *J. Org. Chem.* **1989**, 54, 1766-1769.
28- C. De Stefano, A. Gianguzza and S. Sammartano, *Thermochim. Acta* **1993**, 214, 325-338
29- A. De Robertis, C. Foti, A. Gianguzza and C. Rigano, *J. Solution Chem.* **1996**, 25, 597-606
30- M. S. Henry and M. Z. Hoffman, *J. Phys. Chem.* **1979**, 83, 618-625.
31- G. Accorsi, A. Listorti, K. Yoosaf and N. Armaroli, *Chem. Soc. Rev.* **2009**, 38, 1690-1700
32- A. Bencini, A. Bianchi, E. Garcia-Espana, M. Micheloni, J.A. Ramirez *Coord. Chem. Rev.* **1999**, 188, 97-156.
33- G. Ambrosi, M. Formica, V. Fusi, L. Giorgi, A. Guerri, M. Micheloni, P. Paoli, R. Pontellini, P. Rossi, *Inorg. Chem.* **2007**, 46, 4737-4748.
34- C. Anda, C. Bazzicalupi, A. Bencini, A. Bianchi, P.Fornasari, C. Giorgi, B. Valtancoli, C. Lodeiro, A. J. Parola, F. Pina, *Dalton Trans.* **2003**, 1299-1307.
35- C. R. Groom, I. J. Bruno, M. P. Lightfoot, S. C. Ward, *Acta Cryst.* **2016,** B72, 171-179.
36- G. Arena, R. P. Bonomo, E. Rizzarelli and A. Seminara, *Inorganica Chim. Acta* **1978**, 30, 13-16.
37- G. Anderegg, *Helv. Chim. Acta* **1963**, 46, 2813-2822.
38- N. Türkel and Ç. Şahin, *Chem. Pharm. Bull.* **2009**, 57, 694-699.
39- B. S. Kulkarni, D. Mishra, S. Pal, *J. Chem. Sci.* **2013**, 125, 1247-1258.
40- B. S. Kulkarni, A. Tanwar and S. Pal, in *J. Chem. Sci.* **2007**, 119, 489-499.
41- M. Becatti, A. Bencini, S. Nistri, L. Conti, M. G. Fabbrini, L. Lucarini, V. Ghini, M. Severi, C. Fiorillo, C. Giorgi, L. Sorace, B. Valtancoli and D. Bani, *Sci. Rep.* **2019**, 9, 10320.
42- A. Bettoschi, A. Bencini, D. Berti, C. Caltagirone, L. Conti, D. Demurtas, C. Giorgi, F. Isaia, V. Lippolis, M. Mamusa, S. Murgia, *RSC Adv.* **2015**, 5, 37385-37391.
43- G. Gran, *Analyst* **1952**, 77, 661.
44- P. Gans, A. Sabatini and A. Vacca, *Talanta* **1996**, 43, 1739-1753.
45- L. Alderighi, P. Gans, A. Ienco, D. Peters, A. Sabatini, A. Vacca, *Coord. Chem. Rev.* **1999**, 184, 311-318.
46- R. Montis, A. Bencini, S. J. Coles, L. Conti, L. Fusaro, P. A. Gale, C. Giorgi, P. N. Horton, V. Lippolis, L. K. Mapp, C. Caltagirone, *Chem. Commun.* **2019**, 55, 2745-2748.
47- A. K. Covington, M. Paabo, R. A. Robinson, R. G. Bates, *Anal. Chem.* **1968**, 40, 700-706.
48- C. Bazzicalupi, A. Bencini, E. Berni, A. Bianchi, P. Fornasari, C. Giorgi, A. Masotti, P. Paoletti, B. Valtancoli, *J. Phys. Org. Chem.* **2001**, 14, 432-443.
49- C. Bazzicalupi, A. Bencini, S. Ciattini, C. Giorgi, A. Masoüi, P. Paoletti, B. Valtancoli, N. Navon and D. Meyerstein, *J. Chem. Soc. Dalt. Trans.* **2000**, 2383-2391.
50- Accelrys Software Inc., San Diego, CA, USA.
51- B. R. Brooks, R. E. Bruccoleri, B. D. Olafson, D. J. States, S. Swaminathan and M. Karplus, *J. Comput. Chem.* **1983**.